Structural Analysis of Thin Film Prepared by Cold Remote Nitrogen Plasma Assisted Polymerization

F. Callebert†‡, R. Stephan†, O. Dessaux‡ and P. Goudmand‡

†THOMSON LCC (Subs. of THOMSON CSF), 21850 Saint-Apollinaire - France
‡Laboratoire de Physicochimie, de l'Energétique et des Plasmas, Université des Sciences et Technologies de Lille, 59655 Villeneuve d'Ascq Cedex - France

Abstract

Cold remote nitrogen plasma (CRNP) provides an interesting medium for polymerization of volatile organo-silicon compounds. In such non-ionic medium, etching processes and regazeification of organic moieties are lowered and rapid growth of polymer layer are obtained. Siloxane monomer, mixed with oxygen, have been polymerized in a micro-wave CRNP under a working pressure of 4 to 5 hPa. In particular deposition conditions, IR-TF, XRD and NMR spectroscopy show that the plasma deposited polymeric layers exhibit a high content of silanol groups and cross-linking patterns. Organic species concentrations such as methyl groups decrease with increasing oxygen flow rate leading to a more and more inorganic material. Spin-spin relaxation times determination (by ^1H CPMG-NMR sequences) shows a clear bi-phasic structure which can allow a good understanding of physical properties of the polymeric layers.

Introduction

CRNP assisted polymerization of volatile organosilicon compounds is an interesting preparation technique of thin polysiloxane films. Previous papers [1-5] have shown the important role of oxygen addition in the reactive medium by an important modification of the chemical composition and a drastic change of the electrical properties of the deposit. The aim of this study is to understand the modification of the polymer structure with respect of the amount of oxygen added in mixture with the 1.1.3.3-tetramethyldisiloxane (TMDS), downstream the discharge.

Experimental

The experimental set-up is described elsewhere [3]. A nitrogen plasma is created in a Pyrex tube by a 433 MHz coaxial cavity [6]. The absorbed power is 300 W. Nitrogen is introduced at a constant flow rate of 1.8 slpm under a pressure of 4.8 hPa. TMDS or a mixture of TMDS - O_2 is introduced in the post-discharge plasma at a distance of 1.5 m downstream the discharge. In all this study, TMDS flow rate (Φ_M) is kept at a constant value of 75 sccm. Oxygen flow rate (Φ_{O_2}) is regulated in the range 0-50 sccm. Deposit are obtained on 5 cm^2 aluminium plates. ^{13}C CP-MAS NMR, ^{29}Si MAS-NMR, ^1H MAS and static NMR spectra are performed on a Brücker CPX-100 spectrometer where the Larmor frequency of proton is 100 MHz. For Magic Angle Spinning spectra, the spinning rate is about 3 kHz. All spectra for structural analysis were acquired by a one pulse sequence. The proton spin-lattice relaxation time T_1 have been

Initiation steps

$HMe_2SIOSIMe_2H + [N(^4S)+N(^4S)]$ or $[O(^3P)+O(^3P)]$

$\rightarrow Me_2Si^{\circ}\text{-}O^{\circ} + HMe_2Si^{\circ} + H + N_2$ or O_2 (1)

$\rightarrow HMeSi^{\circ}\text{-}O^{\circ} + HMe_2Si^{\circ} + Me + N_2$ or O_2 (2)

$\rightarrow Me_2Si^{\circ}\text{-}O\text{-}^{\circ}SiMe_2 + 2H + N_2$ or O_2 (3)

Propagation steps

$\equiv SiH + O(^3P)$ or $N(^4S) \rightarrow \equiv Si^{\circ} + OH$ or NH (4)

$\equiv SiMe + [N(^4S)+N(^4S)]$ or $[O(^3P)+O(^3P)]$

$\rightarrow \equiv Si^{\circ} + Me + N_2$ or O_2 (5)

$\equiv Si^{\circ} + O(^3P) + M \rightarrow \equiv Si\text{-}O^{\circ} + M$ (6)

$\equiv Si^{\circ} + {}^{\circ}O\text{-}{}^{\circ}Si= \rightarrow \equiv Si\text{-}O\text{-}{}^{\circ}Si=$ (7)

Termination steps

$\equiv Si^{\circ} + {}^{\circ}O\text{-}Si\equiv \rightarrow \equiv Si\text{-}O\text{-}Si\equiv$ (8)

$\equiv Si^{\circ} + {}^{\circ}OH \rightarrow \equiv Si\text{-}OH$ (9)

Table 1 - Global homogeneous and/or heterogeneous phase reaction mechanisms of a TMDS/O_2 mixture in a CRNP [2]

measured with a $\pi/2\ \tau\ \pi/2$ pulse sequence. Proton relaxation time T_2 calculation have been performed by direct measurement by a Carr-Purcell-Meiboom-Gill sequence in static NMR (CPMG-NMR). This echo-solid sequence have been previously verified on pure distilled water where T_1 equals T_2. ^{29}Si NMR chemical shifts (in ppm) where referenced to liquid tetramethylsilane, a higher shift corresponding to a lower shielding. The crystalline structure of the powder was determined by X-ray diffraction (XRD) method. The chemical composition was investigated using a Perkin-Elmer Fourrier Transformed Infra-Red spectrometer (FTIR).

Results and Discussion

All the XRD patterns of the powders show a broad peak. The crystalline structure of the deposits is, therefore, amorphous. The chemical composition is strongly dependent on the amount of oxygen in mixture with TMDS. Without oxygen, only strong absorption bands of Si-O-Si (1050-1100 cm^{-1}), Si-CH_3 (1250-1270 cm^{-1}) and -CH (2980-2850 and 750-850 cm^{-1}) are evidenced. When oxygen is added, Si-OH (3300-3500 cm^{-1}) and Si-H (2100 cm^{-1}) absorption bands appear. These modifications are understood by different reaction

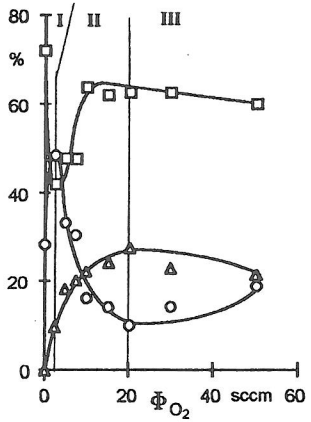

Figure 1 -Evolution of undistinguished linear M^X (○), chain D^X (□) and cross-linking T (△) groups versus Φ_{O_2}

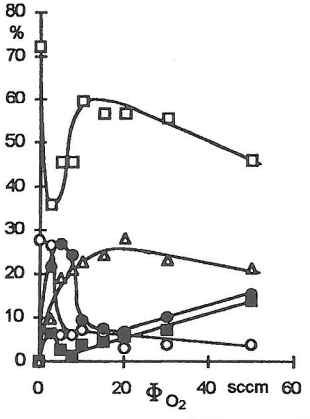

Figure 2 -Evolution of M^{OH} (●), M^H (○), D^{OH} (■)D (□) and T (△) groups versus Φ_{O_2}.

mechanisms (table 1) and are accompanied by a decrease of the volumic mass from 1.5 g/cm^3 for the deposit obtained without oxygen to 1.1 g/cm^3 for the deposit with Φ_{O_2} = 50 sccm.

Because of the very similar δ^{29}_{Si} of siloxane, silazane and siloxazane compounds, unambiguous attribution have been brought by ^{13}C CP-MAS-NMR spectroscopy. ^{13}C CP-MAS-NMR spectra show only two broads peaks, located at 1 ppm and -2.5 ppm with respect to TMS, which are characteristic of polysiloxane structure [10-11]. ^{13}C NMR spectra of silazane or siloxazane have been reported in the range of 4 ppm for D units and 3 ppm for M units [12].

Without oxygen addition, the ^{29}Si MAS-NMR spectrum is only constituted of two single broad peaks at -7.7 ppm (area = 28 %) and -20 ppm (area = 72 %) which correspond to M^H and D group respectively. The calculated stoichiometry of the deposit is $SiO_{0.86}C_2H_{6.27}$. One can assume that the global formulae of the polymer is close to a linear polymethyldisiloxane which have the following form $M^HD_5M^H$ and the theoretical stoichiometry $SiO_{0.857}C_2H_{6.285}$, which is in good agreement with the experimental stoichiometry. The M^H and D line width can result, on one hand, of a specific orientation of the linear chains, leading to a faster spin relaxation and, on the other hand, by an effect of the chemical shifts induced by the increasing distance from the observed D site to the chain end [7]. The absence of quaternary patterns [Q : $(SiO_{1/2})_4$] in the deposit structure suggests that the recombination of silicon atoms, previously evidenced in the gas phase reaction [3], on $\equiv$Si-O$^\bullet$ type radicals is not complete. Figure 1 shows the evolution of undistinguished linear (M^x), chain (D^x) and cross-linking (T^x) groups versus Φ_{O_2}. Three zone can be pointed out. The first one (Zone I) is a transition zone between a linear polymer (Φ_{O_2} = 0 sccm) and a cross-linked polymer (Φ_{O_2} = 2.5 sccm) with a large amount of end groups and short length interreticular chains groups. Between Φ_{O_2} = 2.5 and 20 sccm (Zone II), the density of end groups ($M^x = M^H + M^{OH}$) decreases, correlatively to the increase of the density of chains groups ($D^x = D + D^{OH}$) and cross-linking groups (T) leading to a decrease of order in the polymer structure which is consistent with the decrease of the volumic mass of the deposit. This can be understood by the increase of the global molecular weight of the polymer. In the last zone (Zone III, Φ_{O_2} > 20 sccm) D^x remains high and M^x increases as T decreases. We can assume that in zone III, the molecular weight of the polymer decreases. Figure 2 shows the evolution of M^H, M^{OH}, D, D^{OH} and T patterns versus Φ_{O_2}.

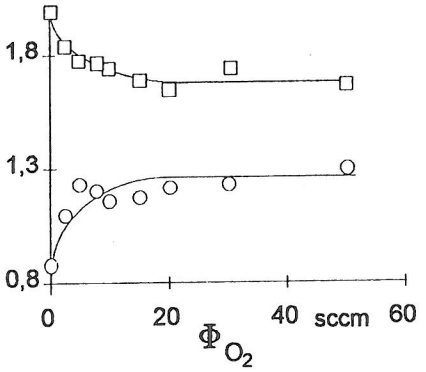

Figure 3 -Evolution of O/Si (○) and C/Si (□) atomic ratios versus Φ_{O_2}.

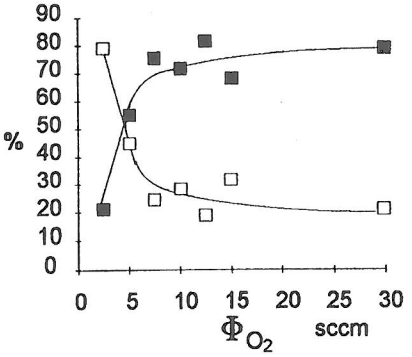

Figure 4 -Evolution of the rigid (■) and the mobile (□) proton phase versus Φ_{O_2}

Several interesting results have been pointed out : no unsubstituted end group (M : + 7 ppm), only single hydroxyl substituted patterns (M^{OH} and D^{OH}), absence of alkoxy substituted groups (M^{OR}, D^{OR} and T^{OR}), a sharp decrease of M^H groups and no Q patterns.

Table 1 gives the suggested reaction pathways of a TMDS/O_2 mixture in a CRNP. The global calculated stoichiometry of deposits is strongly affected by Φ_{O_2} (Fig. 3). C/Si and O/Si atomic ratio reach a constant value in Zone II of 1.68 and 1.2 respectively. The deposit becomes more and more inorganic with an increasing Φ_{O_2} below 20 sccm. We can assume that oxygen addition increases the efficiency of reaction (4) and (5). Those reactions are efficient enough to promote methyl and hydrogen abstraction which is consistent with the decrease of M^H groups density and the increase of T groups density. The absence of M and alkoxy substituted groups in the polymer structure would suggest that no methyl radicals fixation occurs by an homogeneous or heterogeneous reaction. Unsubstituted T patterns may originate from radicals which contain at least one methyl group. Hydrogen abstraction initiation step (3) have to be minimised because of the high remaining of M^H groups in the deposits obtained with low oxygen flow rates. The termination process (9) is in good agreement with NMR data. The parallel evolution of hydroxyled groups would suggest that this process seems to be not selective versus the type of $\equiv Si^\bullet$ radical. In conclusion, those data confirm the role of oxygen in propagation steps by a fixation on $\equiv Si^\bullet$ type radicals.

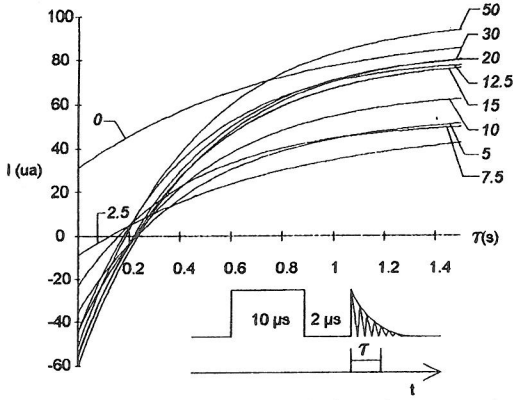

Figure 5 - Evolution of the peak intensity versus the delay τ in T_1 measurement sequence (Φ_{O_2} in sccm)

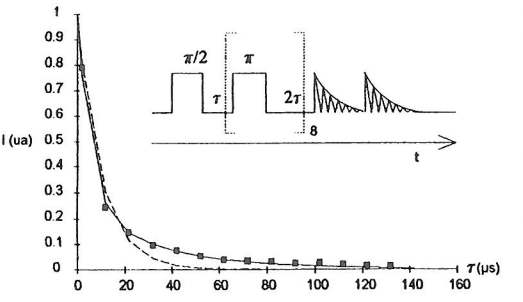

Figure 6 - FID interpolation curves in a CPMG sequence (line : two exponential fit - dotted line : one exponential fit) - Φ_{O_2} = 7.5 sccm

Structure modifications introduced above have been investigated by ^1H MAS and static CPMG-NMR spectroscopy. The MAS spectrum of deposit without oxygen shows a broad peak centred on 0 ppm which have been attributed to the proton in the methyl group. The MAS spectra of deposit with oxygen show the "methyl" zero centred peak and a shoulder located at 5 ppm which can be attributed to hydroxyl groups. The width of the zero centred line sharpens with an increasing oxygen flow rate.

Spin-lattice relaxation time of protons have been measured by using a $\pi/2$ τ $\pi/2$ static NMR sequence and varying the acquisition delay τ (Fig. 5). The evolution of the intensities are plotted versus t and fits the equation :

$$I = A(1 - Be^{-t/T_1}).$$

On another hand, spin-spin relaxation time of protons (T_2) have been studied by performing a CPMG type sequence which allows to avoid

magnetic field heterogeneity. In this sequence, a $\pi/2$ pulse is followed, after a delay τ_2 by a serie of height $\pi 2^*\tau_2$ pulses. The FID is then recorded. The echo-solid signal is adjusted by varying the delay τ_2. Figure 6 shows the intensity of the FID versus τ_2. In the aim to have information on protons phases, a single exponential function have been tested to fit with the standard equation of a single proton phase :

$$I = A_1 e^{-t/T_2}$$

where A = 1 (i.e. 100% of protons in the phase of spin-spin relaxation time T_2). The result of this fit is shown in dotted lines (Fig. 6). The correlation factor is 0.98. A better fit is obtained considering two proton phase which fits with the equation :

$$I = A_1 e^{-t/T'_2} + A_2 e^{-t/T''_2}$$

where A_1 and A_2 are the percentage of protons in the phases T'_2 and T''_2 respectively. In this case, the correlation factor is better than 0.999. Results of spin-lattice and spin-spin relaxation times are gathered in figure 7. The increase of T_2 with Φ_{O_2} can be interpreted by motional narrowing effects on the ^1H static NMR lines which can be occurred by the creeping and sliding of polymer chains. The important spin diffusion effects occurred by dipolar homonuclei interaction between two protons leads to a difficult interpretation of the T_1 evolution.

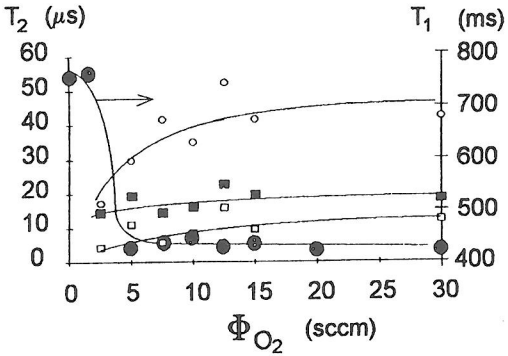

Figure 7 - Evolution of T_2 (□ : rigid, ■ : average, ○ : mobile) and T_{1Z} (●) versus Φ_{O_2}.

The quick relaxing protons (small T_2 values) can be attributed to protons in a rigid phase and the slower relaxing protons to a much mobile phase. The percentage of protons in a rigid and in a mobile phase versus Φ_{O_2} are represented on figure 4.

Without oxygen, the deposit is mostly under a mobile phase. The rigid phase percentage increases and reaches an average value of 70% in zone II. This phase becomes less and less rigid, according to the increase of both T_2 rigid and T_2 mobile. This can be understood by an increase of the interreticular chains length accompanied by shorter end chains. The evolution of protons ratios (Fig. 4) has to be correlated to the evolution of atomic ratios O/Si and C/Si (Fig. 3) which present a sharp evolution in zone I and II and give a good idea of the evolution of the organic and inorganic phases in the plasma polymerized layer structure.

Conclusion

MAS NMR provides a powerful tool for plasma deposit analysis. This technique allows us to strengthen our mechanism model. ^{29}Si MAS-NMR data confirms the fundamental role of oxygen in the polymerization processes by a direct fixation on $\equiv Si^\circ$ type radicals and in methyl and hydrogen abstraction . The absence of Q type groups indicates that silicon atoms do not react completely with oxygen. Unsubstituted T patterns allow us to conclude that only methyled radicals play an active role in the propagation processes. Hydroxyled groups, pointed out by both

^{29}Si and ^{1}H NMR spectroscopy, are good candidates for termination reaction as previously suggested. Rigid and mobile protons environments and a modification of the global structure of the deposit have been pointed out by ^{1}H CPMG-NMR spectroscopy which is in good agreement with previous macroscopic observations.

References

[1] F. Callebert, C. Jama, O. Dessaux and P. Goudmand, 4th TAFT, Dresden, DGM ed., 167 (1994)

[2] F. Callebert, P. Supiot, K. Asfardjani, P. Goudmand, O. Dessaux, J. Laureyns and P. Dhamelincourt, *J. Appl. Polym. Sci.*, **52**, 1595-1606 (1994)

[3] P. Supiot, F. Callebert, O. Dessaux and P. Goudmand, *Plasma Chem. Plasma Proc.*, **3**, 13, (1993)

[4] F. Callebert, P. Supiot, O. Dessaux and P. Goudmand, ISPC 11, 2.6, **4**, 1493 (1993)

[5] F. Callebert, O. Dessaux and P. Goudmand, ISPC 10, 2.3, **3** (1991)

[6] F. Callebert, C. Dupret, O. Dessaux and P. Goudmand, *Int. Pat. Appl.*, WO 92/03591 (1992)

[7] R.K. Harris, J.D. Kennedy and W. McFarlane, in *NMR and the Periodic Table*, Acad. Press, London (1978)

[8] E.K.F. Bahlmann, R.K. Harris and B.J. Say, *Magnetic Resonance in Chemistry*, **31**, 266-267 (1993)

[9] J. Stein, T.M. Leonard and J.F. Smith, *J. Appl. Polym. Sci.*, **47**, 667-675 (1993)

[10] W.L. Earl and D.L. Vanderhart, J. Magn. Res., **48**, 35-54 (1982).

[11] T.M. Duncan, *J. Phys. Chem. Ref. Data*, **16**, 1, 125-151 (1987)

[12] M. Imbenotte, *these*, Universite de Lille (1983)